# A NEW TYPE OF THE QUASI-TEM EIGENMODES IN A RECTANGULAR WAVEGUIDE WITH ONE CORRUGATED HARD WALL

**S. P. Skobelev**

JSC Radiophyzika
10, Geroev Panfilovtsev Street, Moscow 125363, Russia

**P.-S. Kildal**

Chalmers University of Technology
Gothenburg, Sweden

**Abstract**—The problem of determining the eigenmodes of a rectangular waveguide with one hard wall formed by longitudinal corrugations with grooves filled with dielectric is considered. The characteristic equation is derived by using the asymptotic boundary conditions for corrugated surfaces. It is shown analytically that if the groove depth is equal to the value $0.25\lambda/(\varepsilon - 1)^{1/2}$ corresponding to the hard wall condition, the TE eigenmode spectrum of the waveguide contains an infinite set of new non-uniform quasi-TEM modes with different transverse propagation constants in the empty part and identical longitudinal propagation constants equal to the wavenumber $k$. Analytical solution for the case of excitation of the waveguide by a specified source is given, and an example of forming local quasi-TEM waves is considered and discussed.

## 1. INTRODUCTION

The concept of artificial electromagnetic hard and soft surfaces or walls [1, 2], that can be realized by corrugations with grooves filled with dielectric or by strips on a grounded dielectric layer, find important applications in design of conical horn antennas [3–8] and pyramidal horn antennas [9–11]. The studies of the hard and soft surfaces in [12] and [13] also show that they can support wave propagation along the grooves or strips and prohibit wave propagation across them. Such

---

Corresponding author: S. P. Skobelev (skobelev@rol.ru).

properties have allowed the hard and soft surfaces to find a new application associated with design of slot array antennas based on parallel plate waveguides or on rectangular waveguides oversized in one of the transverse directions. Normally, such waveguides have smooth walls as described, for instance, in [14–16] and other references given there. However, it is very difficult to avoid excitation of propagating higher-order modes in the indicated waveguides, and, as a consequence, to achieve high array radiating performance. Another difficulty in such arrays is associated with realizing the phase-steering of the beam in the transverse direction.

To overcome the difficulties indicated above, the authors of [17] have proposed a new type of an oversized rectangular waveguide as an exciter of an array of slots on its upper broad wall. The lower broad wall of the waveguide is loaded with longitudinal corrugations, the grooves of which are filled with dielectric for forming a hard surface structure. Possessing the property of supporting wave propagation in the longitudinal direction along the grooves, such a structure prohibits propagation in the transverse directions, that, according to [17], eliminates reflections of waves from the side walls and thereby eliminates the undesirable propagating modes of higher-order, like those existing in an ordinary rectangular waveguide of oversized width.

Numerical analysis of the fields excited by a single-standing probe and by an array of probes in the waveguide with one hard wall presented in [17] has shown that, if the height of the waveguide is small enough, it can support only one propagating quasi-TEM wave. This useful feature stimulated further studies reported in [18–20]. Numerical analysis of the quasi-TEM wave interaction with linear and planar arrays of slots in the upper wall is presented in [18]. Along with conventional frequency beam-steering in the longitudinal plane, the results of work [19] demonstrate ability of the waveguide to provide the phase-steering of the beam in the transverse plane as well. In paper [20], the authors propose to characterize the quality of the waveguide performance using local quasi-TEM waves similar to those detected earlier in open hard and soft corrugated and strip-loaded planar structures [12]. The detection of the local waves have resulted in invention of more general local gap waveguides [21].

The results of [17–20] have shown good promise of the waveguide with one hard wall for its application in the slot array technology. However, they have been obtained by purely numerical methods without involving the waveguide eigenmodes since, as noted in [20], no solution for them has been obtained. Meanwhile, the knowledge of the waveguide eigenmodes including their structure and propagation constants is useful for better understanding of the features of the

local quasi-TEM wave excitation by the sources in the waveguide and elimination of the other undesirable propagating modes, as well as for more accurate selection of the appropriate design parameters of the waveguide.

The present paper includes Section 2 where derivation and solution of the characteristic equation for the waveguide eigenmodes reported recently in [22] is considered. It also contains analysis of the field structure for the new quasi-TEM eigenmode solutions obtained. The indicated eigenmodes are used in Section 3 for treating the local quasi-TEM waves [20] excited by a vertical electric dipole.

## 2. DETERMINATION OF THE EIGENMODES

### 2.1. Waveguide Geometry and Some Assumptions

Consider a waveguide having a rectangular cross section and arranged in a Cartesian rectangular system of coordinates $0xyz$ as shown in Figure 1. The waveguide is assumed to be infinite (regular) along the $z$ axis. The waveguide width along the $x$ axis is equal to $a$. The cross section has an empty region 1 of height $b$, and a region 2 containing longitudinal corrugations with grooves of depth $d$ and fins of zero thickness. The grooves are filled with dielectric material of relative permittivity $\varepsilon$. It is assumed that the waveguide walls and corrugation fins are perfectly conducting, and the corrugation period (and the groove width, respectively) is much less than the operating wavelength $\lambda$.

The corrugated surface with period approaching zero may be characterized by the asymptotic boundary conditions [23]. Using them, it is possible to show that, similarly to circular longitudinally corrugated waveguides considered in [24] and [25], the eigenmode spectrum of the rectangular waveguide under consideration may be
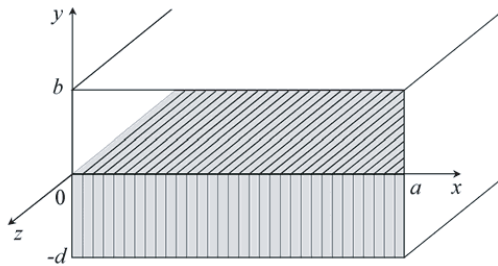


**Figure 1.** Geometry of the waveguide.

split into independent subsystems of TE and TM modes. The latter in this case correspond to those in an ordinary rectangular waveguide of width $a$ and height $b$. If the height is small enough ($b \leq \lambda/2$), as suggested in [17], all the TM modes will be evanescent.

## 2.2. Characteristic Equation for the TE Modes

Assuming that the time dependence suppressed below is taken in the form $\exp(i\omega t)$, we can determine the electric and magnetic field strengths of the TE modes in regions 1 and 2 by formulas [26]

$$\mathbf{E}_{1,2}(x, y, z) = -i\omega\mu_0 \nabla \times (\Pi_{1,2}\mathbf{e}_z) \tag{1}$$

$$\mathbf{H}_{1,2}(x, y, z) = \nabla\nabla \cdot (\Pi_{1,2}\mathbf{e}_z) + k^2\varepsilon_{1,2}\Pi_{1,2}\mathbf{e}_z \tag{2}$$

where $\mu_0$ is the magnetic constant for the free space, $k = 2\pi/\lambda$ is the wavenumber, $\mathbf{e}_z$ is the unit vector along the $z$ axis, $\varepsilon_1 = 1$ for the empty region 1, $\varepsilon_2 = \varepsilon$ for the groove region 2, and $\Pi_{1,2}(x, y, z)$ is the longitudinal component of the Hertz vector which must satisfy the uniform Helmholtz equation for the appropriate region. The solution of that equation for the empty region may be written as

$$\Pi_1(x, y, z) = A_1 e^{-i\gamma z} \cos\frac{m\pi x}{a} \cos\alpha(b - y) \tag{3}$$

where $A_1$ is an unknown amplitude coefficient,

$$\gamma = \sqrt{k^2 - (m\pi/a)^2 - \alpha^2} \tag{4}$$

is the longitudinal propagation constant, $\alpha$ is the transverse propagation constant along the $y$ axis, and $m$ is an integer number determining the transverse propagation constant $m\pi/a$ along the $x$ axis.

Substituting (3) in (1) and (2), we obtain

$$E_{1x} = -i\omega\mu_0\alpha A_1 e^{-i\gamma z} \cos\frac{m\pi x}{a} \sin\alpha(b - y) \tag{5}$$

$$E_{1y} = -i\omega\mu_0\frac{m\pi}{a}A_1 e^{-i\gamma z} \sin\frac{m\pi x}{a} \cos\alpha(b - y) \tag{6}$$

$$H_{1x} = i\gamma\frac{m\pi}{a}A_1 e^{-i\gamma z} \sin\frac{m\pi x}{a} \cos\alpha(b - y) \tag{7}$$

$$H_{1y} = -i\gamma\alpha A_1 e^{-i\gamma z} \cos\frac{m\pi x}{a} \sin\alpha(b - y) \tag{8}$$

$$H_{1z} = (k^2 - \gamma^2)A_1 e^{-i\gamma z} \cos\frac{m\pi x}{a} \cos\alpha(b - y) \tag{9}$$

and $E_{1z} = 0$. As we can see, the electric field components (5) and (6) vanish on the upper and side walls, respectively, as it just must be for the perfectly conducting walls.
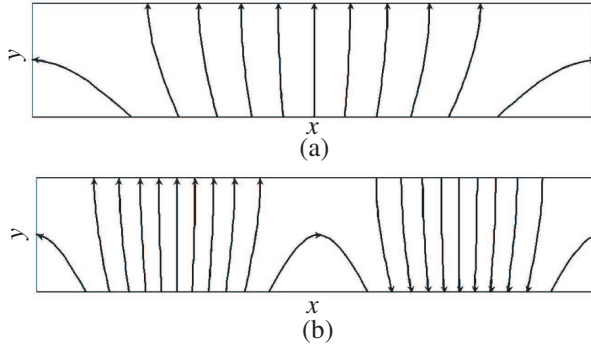
**Figure 2.** Electric field strength lines of the quasi-TEM modes for $m = 1$ (a) and $m = 2$ (b).
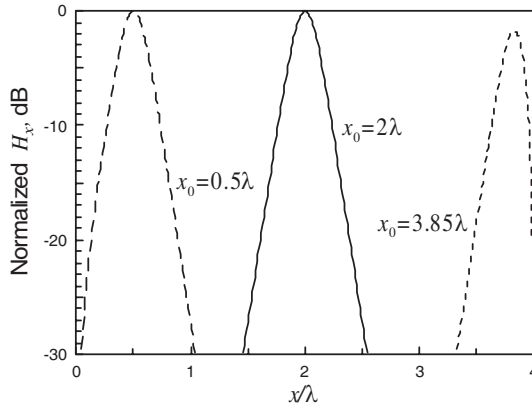


**Figure 3.** Distributions of the normalized magnetic field component $H_x$ in dB across the upper wall for different dipole positions $x_0$.

Since the width of each groove is close to zero, the function $\Pi_2(x, y, z)$ satisfying the uniform Helmholtz equation in one of the grooves may be represented in the form

$$\Pi_2(x, y, z) = A_2 e^{-i\gamma z} \cos \beta(d + y) \qquad (10)$$

where $\beta$ is the transverse propagation constant related to the longitudinal one by formula

$$\gamma = \sqrt{k^2 \varepsilon - \beta^2} \qquad (11)$$

taking into account the fact that the longitudinal propagation constant must be identical for both regions of the cross section, and $A_2$ is an amplitude coefficient depending on the position of the groove.

Substitution of (10) in (1) and (2) yields the expression for the fields in the groove

$$E_{2x} = i\omega\mu_0\beta A_2 e^{-i\gamma z} \sin\beta(d+y) \qquad (12)$$

$$H_{2y} = i\gamma\beta A_2 e^{-i\gamma z} \sin\beta(d+y) \qquad (13)$$

$$H_{2z} = (k^2\varepsilon - \gamma^2)A_2 e^{-i\gamma z} \cos\beta(d+y) \qquad (14)$$

while $E_{2y} = E_{2z} = H_{2x} = 0$. Note that formula (12) accounts for satisfaction of the boundary conditions for the groove bottom and $E_{2y} = 0$ on the groove walls formed by the fins.

According to the asymptotic boundary conditions [23] for the corrugated surface, the transverse electric field strength component $E_x$ and longitudinal magnetic field strength component $H_z$ must be continuous on the boundary. Therefore, equating (5) and (12) as well as (9) and (14) at $y = 0$, we obtain the equations

$$\alpha A_1 \cos\frac{m\pi x}{a} \sin\alpha b + \beta A_2 \sin\beta d = 0 \qquad (15)$$

$$(k^2 - \gamma^2)A_1 \cos\frac{m\pi x}{a} \cos\alpha b - (k^2\varepsilon - \gamma^2)A_2 \cos\beta d = 0 \qquad (16)$$

Determining the amplitude $A_2$ from (15) by formula

$$A_2 = -A_1 \frac{\alpha\sin\alpha b}{\beta\sin\beta d} \cos\frac{m\pi x}{a} \qquad (17)$$

and substituting it in (16), we obtain the characteristic equation

$$[\beta^2 - k^2(\varepsilon-1)]\frac{\cos\alpha b}{\alpha\sin\alpha b} + \frac{\beta\cos\beta d}{\sin\beta d} = 0 \qquad (18)$$

where we have taken into account formulas (4) and (11). The characteristic Equation (18) may be solved with respect to $\beta$ and accounting for relation

$$\alpha = \sqrt{\beta^2 - (m\pi/a)^2 - k^2(\varepsilon-1)} \qquad (19)$$

obtained with using (4) and (11).

## 2.3. The Quasi-TEM Modes

In case of $m = 0$, when the fields in the waveguide do not depend on $x$, we, accounting for (19), may rewrite Equation (18) in the form

$$\frac{\cos\alpha b\sin\beta d}{\beta} + \frac{\sin\alpha b\cos\beta d}{\alpha} = 0. \qquad (20)$$

The Equation (20) corresponds to the horizontally polarized $\text{TE}_{0n}$ modes ($n = 1, 2, \ldots$) of a rectangular waveguide partially filled with

a dielectric layer of thickness $d$ (without the metal fins) lying on the lower wall [26, 27]. Propagation of these modes is undesirable for the purposes considered in [17–20]. Therefore, the parameters $b$ and $d$ should be chosen small enough to keep all the $TE_{0n}$ modes below cutoff at specified permittivity $\varepsilon$ of the groove filling.

Both Equation (20) and Equation (18) at $m > 0$ can in general case be solved only numerically. However, there is an exception. If the depth $d$ and permittivity $\varepsilon$ of the grooves satisfy the well known hard wall condition [9]

$$d = \frac{\lambda}{4\sqrt{\varepsilon - 1}}, \tag{21}$$

the first root of (18) at $m > 0$ is determined analytically as

$$\beta_{m1} = k\sqrt{\varepsilon - 1} \tag{22}$$

independently of $m$ and transverse constant $\alpha$. The latter is then determined from (19) by formula

$$\alpha_{m1} = i\frac{m\pi}{a} \tag{23}$$

while the longitudinal propagation constant (4) or (11) is exactly equal to the wavenumber, i.e.,

$$\gamma_{m1} = k. \tag{24}$$

The transverse electric and magnetic fields corresponding to the solution found above may be written in the form

$$\mathbf{E}_{m1}^{\pm}(x, y, z) = \mathbf{\Phi}_{m1}(x, y)e^{\mp ikz} \tag{25}$$

$$\mathbf{H}_{\tau m1}^{\pm}(x, y, z) = \pm\frac{1}{\eta_0}[\mathbf{e}_z \times \mathbf{E}_{m1}^{\pm}(x, y, z)] \tag{26}$$

where the common amplitude coefficient is omitted, the upper and lower signs in superscripts correspond to the waves propagating in the positive and negative direction along the $z$ axis, respectively, $\eta_0$ is the wave impedance for the free space, and

$$\mathbf{\Phi}_{m1}(x, y) = \frac{1}{N_{m1}} \begin{cases} -\mathbf{e}_x \cos\dfrac{m\pi x}{a} \sinh\dfrac{m\pi(b - y)}{a} \\ +\mathbf{e}_y \sin\dfrac{m\pi x}{a} \cosh\dfrac{m\pi(b - y)}{a}, \\ 0 \le y \le b, \\ -\mathbf{e}_x B_m \cos\dfrac{m\pi x}{a} \sin[\beta_{m1}(d + y)], \\ -d \le y \le 0, \end{cases} \tag{27}$$

is the orthonormalized transverse wave function where $B_m = \sinh(m\pi b/a)$ and

$$N_{m1} = \frac{a}{2}\sqrt{\frac{1}{m\pi}\sinh\frac{2m\pi b}{a} + \frac{d}{a}\sinh^2\frac{m\pi b}{a}} \qquad (28)$$

is a normalizing coefficient, at which the orthogonality relation for (27) takes the form

$$\int\limits_{0}^{a}\int\limits_{-d}^{b} \mathbf{\Phi}_{m'1}(x,y)\cdot\mathbf{\Phi}_{m1}(x,y)dxdy = \delta_{m'm} \qquad (29)$$

with $\delta_{m'm}$ being the Kronecker symbol.

The non-zero longitudinal component of the magnetic field in the grooves is

$$H^{\pm}_{2zm1}(x,y,z) = \frac{i\sqrt{\varepsilon - 1}}{\eta_0}B_m e^{\mp i\gamma z}\cos\frac{m\pi x}{a}\cos\beta_{m1}(d+y). \qquad (30)$$

The solutions represented by (25) through (30) correspond to the quasi-TEM eigenmodes whose fields are purely transverse in the empty region 1 only. The equations of the electric field strength lines there are solutions of the differential equation $dy/dx = E_y/E_x$. For the first harmonic $(m = 1)$, the solution for a line going between the upper wall and the plane of corrugations at $y = 0$ may be expressed as

$$x(y) = \frac{a}{\pi}\arcsin\sqrt{1 - \frac{\cos^2(\pi x_b/a)}{\cosh^2[\pi(b-y)/a]}} \qquad (31)$$

where $0 \leq x_b = x(b) \leq a/2$ corresponds to a specified initial point on the upper wall. The solution for a line going between the left side wall and the plane of corrugations may be represented as

$$y(x) = b - \frac{a}{\pi}\ln\left(\sqrt{u^2 - 1} + u\right) \qquad (32)$$

where

$$u(x) = \frac{\cosh[\pi(b-y_0)/a]}{\cos(\pi x/a)}$$

and $0 \leq y_0 = y(0) \leq b$ corresponds to a specified initial point on the left side wall. The strength lines in the right half of the waveguide cross section are mirror images of the lines described by Equations (31) and (32). A picture of the strength lines in the empty region for $a = 0.5\lambda$ and $b = 0.1\lambda$ is shown in Figure 2(a). This structure is basic for constructing the strength lines for arbitrary $m > 1$. Like for an ordinary rectangular waveguide, the cross section in this case is

divided by rectangular cells of dimensions $(a/m) \times b$, and each cell is filled in with the basic structure appropriately compressed along the $x$ axis, while the directions of the lines in the adjacent cells must be opposite. An example of the strength lines for $m = 2$ is presented in Figure 2(b).

Note, that the *non-uniform* quasi-TEM waves described above represent a new type of the eigenmodes different from the well known *uniform* quasi-TEM modes existing in the waveguides and horns of rectangular (or square) cross section considered in [9–11]. The new solution obtained above allows us to refine some claims made in [17–20] regarding "killing" of higher order modes. The spectrum of the propagating eigenmodes in an ordinary rectangular waveguide of small height and oversized (of a few wavelengths) width comprises the dominant $TE_{10}$ mode and a few next $TE_{m0}$ modes of higher order. All the other modes are evanescent. The remarkable property of the longitudinally corrugated hard surface on one waveguide wall detected above consists in transforming all the propagating and evanescent $TE_{m0}$ modes, which are non-degenerate, into an infinite set of degenerate quasi-TEM modes with different transverse propagation constants and identical longitudinal propagation constants equal to the wavenumber $k$. Note, that this case of degeneracy with respect to the longitudinal constants only differs from the classical case where different degenerate modes have both identical transverse constants and identical longitudinal constants, as, for instance, it takes place for a $TE_{mn}$ mode and a $TM_{mn}$ mode in an ordinary rectangular waveguide.

## 2.4. Other Modes and Frequencies

To provide the situation when the quasi-TEM modes are propagating while all the other modes are evanescent as required in the waveguide slot arrays, it is necessary to select an appropriate value for the height $b$ of the empty part of the waveguide cross section. This is done here by analyzing the numerical solutions obtained for the characteristic Equation (18) and its partial case (20) under the hard wall condition (21). The analysis has shown that when the height $b$ increases from zero, the next propagating mode after the quasi-TEM modes is the $TE_{01}$ mode with propagation constants determined from solution of Equation (20). For instance, maximum $b$ at which that mode is still evanescent are $0.1191\lambda$, $0.1868\lambda$, and $0.2079\lambda$ for permittivity of groove filling in the hard wall $\varepsilon = 2$, 5, and 10, respectively. The groove depths determined by (21) at the indicated values of the permittivity are equal to $\lambda/4$, $\lambda/8$, and $\lambda/12$, respectively.

The cut-off values of $b$ for the $TE_{12}$ mode (corresponding to the 2nd root of (18) at $m = 1$) at large waveguide width $a$ only slightly

exceed the values indicated above for the $TE_{01}$ mode. For instance, the indicated values for $\varepsilon = 2, 5,$ and $10$ are equal to $0.1218\lambda$, $0.1894\lambda$, and $0.2105\lambda$, respectively. Thus, if the $TE_{01}$ mode is evanescent at a selected value of $b$, all the other higher order modes will be evanescent as well.

One more issue of importance is behavior of the $TE_{m1}$ eigenmodes at frequencies $f$ different from the TEM frequency $f_{TEM}$ at which the hard wall condition (21) is satisfied. To show the degree of changing the propagation constants, let's consider an example of the waveguide with parameters $a = 4\lambda$, $b = 0.15\lambda$, $t = 0.125\lambda$, and $\varepsilon = 5$, where $\lambda$ corresponds to $f_{TEM}$. The first root $\beta_{m1}$ of Equation (18) determined numerically at frequency $f = 0.95f_{TEM}$, as well as the corresponding longitudinal propagation constant $\gamma_{m1}$ are equal to $\beta_{m1} = 2.000530k$ and $\gamma_{m1} = 0.998939k$ for $m = 1$, and $\beta_{m1} = 2.029457k$ and $\gamma_{m1} = 0.938778k$ for $m = 10$. Similar results at frequency $f = 1.05f_{TEM}$ are $\beta_{m1} = 1.999356k$ and $\gamma_{m1} = 1.001287k$ for $m = 1$, and $\beta_{m1} = 1.971536k$ and $\gamma_{m1} = 1.055010k$ for $m = 10$. Note, that the corresponding values at the TEM frequency are equal to $\beta_{m1} = 2k$ and $\gamma_{m1} = k$ for any $m > 0$. Thus, the propagation constants of the operating $TE_{m1}$ modes at frequencies different from $f_{TEM}$ become different, and this is just the reason of some spraying of the local modes in the process of their propagation along the waveguide demonstrated in [20].

## 3. EXCITATION OF THE LOCAL QUASI-TEM WAVES

A remarkable property of the waveguide with one corrugated hard wall shown in Figure 1 is its ability of forming localized quasi-TEM waves as shown in [17–20]. The problem of excitation of them by specified sources has been solved in the indicated papers by numerical methods. We consider here an analytical solution based on a general approach considered in a number of text books. We will follow the technique described in [28]. Let **E** and **H** are strengths of electric and magnetic fields excited in the waveguide by, for instance, an elementary vertical electric dipole arranged in the point $\{x_0,\ y_0,\ z_0\}$ with $0 < x_0 < a$, $0 < y_0 < b$, and $z_0 = 0$. The current density of this source is given by formula

$$\mathbf{j}(x,y,z) = Il\mathbf{e}_y\delta(x - x_0)\delta(y - y_0)\delta(z) \qquad (33)$$

where $I$ is the current and $l$ is the length of the dipole ($l \ll \lambda$). To determine the indicated fields **E** and **H**, we apply the Lorentz

reciprocity theorem [26], page 325, or [28], page 290:

$$\oint_S (\mathbf{E} \times \mathbf{H}_p^- - \mathbf{E}_p^- \times \mathbf{H}) \cdot \mathbf{n} dS = \int_V \mathbf{j} \cdot \mathbf{E}_p^- dV \qquad (34)$$

where $\mathbf{E}_p^-$ and $\mathbf{H}_p^-$ are the orthonormalized fields of a $p$th waveguide eigenmode propagating or evanescent in the negative direction of the $z$ axis, $p$ is its ordinal number depending on appropriate indices, and $V$ is a volume of an interior part of the waveguide bounded by surface $S$ with outer unit normal $\mathbf{n}$. The surface consists of two cross sections $S^+$ and $S^-$ situated at distance $\pm L$ from the origin, as well as a part of the waveguide walls $S^{wall}$ between the indicated cross sections.

Since the tangential electric field vanishes on the waveguide wall, the integral over $S^{wall}$ in (34) is equal to zero. The fields on the surfaces $S^\pm$ are superpositions of the waveguide eigenmodes

$$\mathbf{E}(x, y, \pm L) = \sum_q B_q^\pm \mathbf{E}_q^\pm(x, y, \pm L) \qquad (35)$$

$$\mathbf{H}(x, y, \pm L) = \sum_q B_q^\pm \mathbf{H}_q^\pm(x, y, \pm L) \qquad (36)$$

going from the source with unknown amplitudes $B_q^\pm$. Substituting (33), (35), and (36) in (34) and using the orthogonality of the waveguide eigenmodes, we find

$$B_p^+ = -\frac{\eta_0 I l}{2} E_{yp}^-(x_0, y_0, 0) \qquad (37)$$

while the amplitude $B_p^-$ is determined similarly by replacing the auxiliary fields $\mathbf{E}_p^-$ and $\mathbf{H}_p^-$ in (34) by $\mathbf{E}_p^+$ and $\mathbf{H}_p^+$, respectively.

Using (37), we can now determine the $x$-component of the total magnetic field of the quasi-TEM waves excited on upper waveguide wall by the specified source (33). The indicated component is of interest because it corresponds to the longitudinal current exciting the transverse slots on the upper wall as considered in [17–20]. Extracting the quasi-TEM part from (36) and accounting for (25)–(27), we obtain

$$H_{x,TEM}^\pm(x, b, z) =$$

$$\pm \frac{Il}{2} e^{\mp ikz} \times \sum_{m=1}^{\infty} \frac{1}{N_{m1}^2} \sin \frac{m\pi x_0}{a} \cosh \frac{m\pi(b - y_0)}{a} \sin \frac{m\pi x}{a} \qquad (38)$$

Some examples of distributions of the field (38) across the wall in the waveguide with $a = 4\lambda$, $b = 0.15\lambda$, $d = 0.125\lambda$, and $\varepsilon = 5$ are presented in Figure 3 where different curves correspond to different positions of the dipole over $x$ for constant $y_0 = 0.07\lambda$. The curves

have been normalized on the maximum of the field formed by the dipole arranged at $x_0 = 2\lambda$. These curves obtained from the explicit expression (38) confirm the results [17–20] on forming the quasi-TEM waves localized at longitudinal lines corresponding to specified sources. We can also see that the local waves are effectively excited almost for any position of the source with respect to the side walls. The amplitude only decreases if the source is arranged very close to the side wall. This feature allows one to manage without special means for equalizing the amplitude distributions of the local waves excited by a transverse linear array of sources as considered in [19].

## 4. CONCLUSION

The paper presents an analytical study of eigenmodes in a rectangular waveguide with one hard wall formed by longitudinal corrugations with grooves filled with dielectric. The study has been based on application of the asymptotic boundary conditions for corrugated surfaces valid when the period of corrugations is much less than the operating wavelength.

The assumption indicated above allowed derivation of a characteristic equation for propagation constants of the TE eigenmodes. Analysis of the characteristic equation has shown that if the groove depth satisfies the hard wall condition, the TE mode spectrum of the waveguide contains an infinite set of non-uniform quasi-TEM modes with different transverse propagation constants in the empty part of the cross section and identical longitudinal propagation constants equal to the wavenumber.

The new solution found as a result of the analysis allows refining the claim made in [20] regarding killing the higher order modes. In fact, the longitudinally corrugated hard wall transforms all the propagating and evanescent $TE_{m0}$ eigenmodes of an ordinary oversized rectangular waveguide into an infinite set of the quasi-TEM eigenmodes having identical longitudinal propagation constants. A superposition of such modes can form quasi-TEM waves localized at a longitudinal line corresponding to a specified source as was shown numerically in [17–20] and analytically in the present study.

The solution of the characteristic equation derived in the paper allows making correct choice of the waveguide dimensions to provide the absence of the propagating modes of higher order undesirable when using the waveguide as an exciter of array of slot radiators.

Finally, it should be noted that the hard wall can also be realized by a dielectric layer screened at one side and loaded with longitudinal strips at another one. However, analysis of a characteristic equation for

such a case has shown that the waveguide with one hard strip-loaded wall has no TE eigenmodes with identical longitudinal propagation constants similar to those detected as a result of the study carried out above.

## ACKNOWLEDGMENT

## REFERENCES

1. Kildal, P.-S., "Definition of artificially soft and hard surfaces for electromagnetic waves," *Electron. Lett.*, Vol. 24, 168–170, 1988.
2. Kildal, P.-S., "Artificially soft and hard surfaces in electromagnetics," *IEEE Trans. Antennas and Propagat.*, Vol. 38, 1537–1544, 1990.
3. Lier, E. and P.-S. Kildal, "Soft and hard horn antennas," *IEEE Trans. Antennas and Propagat.*, Vol. 36, 1152–1157, 1988.
4. Lier, E., "Analysis of soft and hard strip-loaded horns using a circular cylindrical model," *IEEE Trans. Antennas and Propagat.*, Vol. 38, 783–793, 1990.
5. Skobelev, S. P. and P.-S. Kildal, "Analysis of conical quasi-TEM horn with a hard corrugated section," *IEEE Trans. Antennas and Propagat.*, Vol. 51, 2723–2731, 2003.
6. Skobelev, S. P. and P.-S. Kildal, "Mode-matching modeling of a hard conical quasi-TEM horn realized by an EBG structure with strips and vias," *IEEE Trans. Antennas and Propagat.*, Vol. 53, 139–143, 2005.
7. Skobelev, S. P., "An approach to the design of a two-frequency hard horn," *Journal of Communications Technology and Electronics*, Vol. 50, 1272–1276, 2005.
8. Skobelev, S. P. and P.-S. Kildal, "Modal solutions in dual-depth longitudinally corrugated hard waveguide," *IET Microwaves, Antennas & Propagation*, Vol. 1, 827–831, 2007.
9. Kildal, P.-S., "Bandwidth of a square hard horn," *IEE Proc. H*, Vol. 135, 275–278, 1988.
10. Skobelev, S. P. and P.-S. Kildal, "Characteristics of arrays of stepped horns with dielectric-loaded walls in one plane," *Journal*

*of Communications Technology and Electronics*, Vol. 45, 964–969, 2000.

11. Epp, L. W., D. J. Hoppe, and D. T. Kelley, "A TE/TM modal solution for rectangular hard waveguides," *IEEE Trans. Miscrowave Theory Techniques*, Vol. 54, 1048–1054, 2006.

12. Sipus, Z., H. Merkel, and P.-S. Kildal, "Green's functions for planar soft and hard surfaces derived by asymptotic boundary conditions," *IEE Proc. H*, Vol. 144, 321–328, 1997.

13. Kildal, P.-S. and A. Kishk, "EM Modeling of surfaces with STOP or GO characteristics — artificial magnetic conductors and soft and hard surfaces," *ACES Journal*, Vol. 18, 32–40, 2003.

14. Hirokawa, J. and M. Ando, "Efficiency of 76-GHz post-wall waveguide-fed parallel-plate slot arrays," *IEEE Trans. Antennas and Propagat.*, Vol. 48, 1742–1745, 2000.

15. Sierra-Castaner, M., M. Vera-Isasa, M.Sierra-Perez, and J. L. Fernandez-Jambrina, "Double-beam parallel-plate slot antenna," *IEEE Trans. Antennas and Propagat.*, Vol. 53, 977–984, 2005.

16. Ettorre, M., A. Neto, G. Gerini, and S. Maci, "Leaky-wave slot array antenna fed by a dual reflector system," *IEEE Trans. Antennas and Propagat.*, Vol. 56, 3143–3149, 2008.

17. Alfonso, E., A. Valero-Nogueira, J. I. Herranz, and D. Sánchez, "Oversized waveguides for TEM propagation using hard surfaces," *Proc. of 2006 IEEE AP-S Symposium*, 1193–1196, Albuquerque, NM, July 9–14, 2006.

18. Alfonso, E., A. Valero-Nogueira, J. I. Herranz, and V.-M. Rodrigo-Peñarrocha, "Slot array fed by an oversized TEM waveguide," *Proc. of the 1st European Conference on Antennas and Propagation: EuCAP 2006*, Nice, France, November 6–10, 2006.

19. Valero-Nogueira, A., E. Alfonso, J. I. Herranz, and M. Baquero, "Planar slot-array antenna fed by an oversized quasi-TEM waveguide," *Microwave and Optical Technology Letters*, Vol. 49, 1875–1877, 2007.

20. Alfonso, E., P.-S. Kildal, A. Valero, and J. I. Herranz, "Study of local quasi-TEM waves in oversized waveguides with one hard wall for killing higher order global modes," *Proc of 2008. IEEE AP-S Symposium*, San Diego, CA, July 2008.

21. Kildal, P.-S., E. Alfonso, A. Valero-Nogueira, and E. Rajo-Iglesias, "Local metamaterial-based waveguides in gaps between parallel metal plates," *Antennas and Wireless Propagation Letters*, Vol. 8,

84–87, 2009.

22. Skobelev, S. P. and P.-S. Kildal, "Analysis of global eigenmodes in an oversized rectangular waveguide with a hard surface on one broad wall for planar slot array antenna applications," *Proc. of the 3rd European Conference on Antennas and Propagation: EuCAP 2009*, Berlin, Germany, March 23–27, 2009.

23. Kildal, P.-S., A. Kishk, and Z. Sipus, "Asymptotic boundary conditions for strip-loaded and corrugated surfaces," *Microwave and Optical Technology Letters*, Vol. 14, 99–101, 1997.

24. Scharten, T., J. Nellen, and F. van den Bogaart, "Longitudinally slotted conical horn antenna with small flare angle," *IEE Proc. H*, Vol. 128, 117–123, 1981.

25. Aly, M. S. and S. F. Mahmoud, "Propagation and radiation behaviour of a longitudinally slotted horn with dielectric-filled slots," *IEE Proc. H*, Vol. 132, 477–479, 1985.

26. Balanis, C. A., *Advanced Engineering Electromagnetics*, Wiley, New York, 1989.

27. Yegorov, Y. V., *Partially Filled Rectangular Waveguides*, Soviet Radio Press, Moscow, 1967 (Russian).

28. Vainshtein, L. A., *Electromagnetic Waves*, 2nd edition, Radio and Communications Press, Moscow, 1988 (Russian).